Retinal Vascularization Rate Predicts Retinopathy of Prematurity and Remains Unaffected by Low-Dose Bevacizumab Treatment

EMER CHANG[#], AMANDEEP JOSAN[#], RAVI PUROHIT, SHER A. ASLAM, CAROLINE HARTLEY, CHETAN K. PATEL, AND KANMIN XUE

• PURPOSE: To assess the rate of retinal vascularization derived from ultra-widefield (UWF) imaging-based retinopathy of prematurity (ROP) screening as predictor of type 1 ROP and characterize the effect of anti–vascular endothelial growth factor (anti-VEGF) therapy on vascularization rate.
• DESIGN: Retrospective, consecutive cohort study.
• SUBJECTS: The study included 132 eyes of 76 premature infants with a mean gestational age (GA) of 26.0 (±2.0 SD) weeks and birthweight (BW) of 815 (±264) g, who underwent longitudinal UWF imaging for ROP screening, at a level 3 neonatal unit in Oxford, United Kingdom.
• METHODS: The extent of retinal vascularization on each UWF image was measured as the ratio between "disc-to-temporal vascular front" and "disc-to-fovea" distance along a straight line bisecting the vascular arcades. Measurements from ≥3 time points plotted against postmenstrual age (PMA) enabled calculation of temporal vascularization rate (TVR) for each eye. Using TVR, GA, and BW as predictors, a machine learning model was created to classify eyes as either group AB (no ROP and type 2 ROP) or group C (type 1 ROP). The model was validated in a withheld cohort of 32 eyes (19 infants), of which 8 eyes (5 infants) required treatment. TVR in 37 eyes (20 infants) was compared before and after ultra-low-dose (0.16 mg) intravitreal bevacizumab treatment.
• MAIN OUTCOME MEASURES: The rate of retinal vascularization was determined.
• RESULTS: Slower retinal vascularization correlated with increasing ROP severity, with TVR being 29% slower in group C eyes (n=50) than group AB eyes (n=33 no ROP and n=49 type 2 ROP) ($P = .04$). Our model correctly predicted ROP outcomes of 30/32 eyes, achieving a balanced accuracy of 95.8%. No significant change in TVR was found before and after bevacizumab treatment with mean posttreatment imaging follow-up of 7.7 (±7.9) weeks ($P = .60$ right eyes, $P = .71$ left eyes).
• CONCLUSIONS: UWF imaging-based ROP screening enables quantification of retinal vascularization rate, which can provide early prediction of type 1 ROP independent of BW and GA. Rate of physiological retinal vascularization does not appear to be significantly affected by ultra-low-dose anti-VEGF treatment, which has significant implications for the development of peripheral avascular retina and timing of anti-VEGF intervention to prevent disease progression in high-risk infants. (Am J Ophthalmol 2025;275: 74–87. © 2025 Published by Elsevier Inc.)

Retinopathy of prematurity (ROP) is a leading cause of childhood blindness worldwide.[1] It is characterized by aberrant retinal vascular development that progresses through 2 main phases: (1) delayed retinal vascularization in phase 1 results in peripheral avascular retina (PAR), which stimulates release of angiogenic factors, followed by (2) a vasoproliferative phase 2 associated with extraretinal neovascularization and subsequent tractional retinal detachment.[2-4] ROP causes visual impairment in more than 30 000 preterm babies globally,[5] with rising incidence over the past decades owing to improved survival of extreme preterm infants (eg, those born as early as 22 weeks).[6]

Timely detection of ROP enables treatment by anti–vascular endothelial growth factor (anti-VEGF) therapy or laser photocoagulation to prevent sight loss.[7] Low gestational age (GA <31 weeks) and birthweight (BW ≤1500 g) are major risk factors for developing ROP, thus con-

AJO.com Supplemental Material available at AJO.com.

Emer Chang and Amandeep Josan contributed equally as co-first authors.
Accepted for publication February 10, 2025.

From the Oxford Eye Hospital, Oxford University Hospitals NHS Foundation Trust (E.C., A.J., R.P., S.A.A., C.K.P., K.X.), Oxford, UK; Nuffield Laboratory of Ophthalmology, Nuffield Department of Clinical Neurosciences, University of Oxford (A.J., K.X.), Oxford, UK; Department of Paediatrics, University of Oxford (C.H.), Oxford, UK; Ophthalmology Department, Great Ormond Street Hospital for Children NHS Foundation Trust (K.X.), London, UK

Inquiries to Kanmin Xue, Level 6 West Wing, Nuffield Department of Clinical Neurosciences, University of Oxford, John Radcliffe Hospital, Headley Way, Oxford OX3 9DU, United Kingdom.; e-mail: kanmin.xue@eye.ox.ac.uk

[#] EC and AJ contributed equally as co-first authors.

0002-9394/$36.00
https://doi.org/10.1016/j.ajo.2025.02.040

stitute the inclusion criteria for ROP screening.[7] Other risk factors include oxygen supplementation, slow postnatal weight gain, sepsis, and respiratory distress.[8,9] Although many of these factors are interlinked, their individual predictive power for ROP occurrence remains poorly defined.

The current ROP grading system (based primarily on zones I-III, stages 0-5, and normal to plus disease spectrum)[10] is applied during ROP screening examinations using either binocular indirect ophthalmoscopy (BIO) or digital retinal imaging. BIO is a technically demanding skill in premature infants and is mainly focused on detecting features of vasoproliferation, such as stage 3 (elevated neovascular ridge) and plus disease (vessel dilation and tortuosity), which pertains to the ROP treatment threshold. However, indirect ophthalmoscopy is less suited to assessing delayed retinal vascularization, which can only be gleaned approximately from 33 to 34 weeks postmenstrual age (PMA) at which stage vessels reach the edge of zone I or zone II.[11]

Wide-field retinal imaging could enable accurate assessment and longitudinal monitoring of the rate of retinal vascularization from birth. Contact retinal imaging such as the 130° RetCam 3 Wide-field Digital Imaging System (Natus Medical Inc., USA) provides limited ability to visualize the posterior pole and far peripheral retina in a single imaging field.[12-15] Noncontact 200° ultra-widefield (UWF) retinal imaging (eg, Optomap; Optos plc., UK) could potentially overcome this limitation to enable consistent and accurate quantification of the rate of retinal vascularization over time. We have previously demonstrated the utility of UWF imaging for ROP assessment with the infants being held to the camera using the "flying baby" technique.[16] We have more recently transitioned from BIO examination to UWF imaging as the default method of ROP screening at our level 3 neonatal unit using an Optos California imaging system mounted on a mobile trolley with onboard battery.

In this study, we aimed to devise a practical method for measuring the rate of retinal vascularization in a retrospective analysis of serial UWF images obtained from routine ROP screening. Using retinal vascularization rate, GA, and BW as predictors, we aimed to create a machine learning–based gradient-boosting model for predicting ROP requiring treatment (type 1 ROP), which demonstrates high accuracy in a separate validation data set.

The presence of PAR has been reported in a high proportion (91%-100%) of infants who have received intravitreal anti-VEGF therapy for ROP.[17,18] However, the causal relationship between anti-VEGF treatment and PAR remains unclear because PAR may be associated with ROP itself. Nonetheless, in clinical practice, concerns about potential vascular arrest following anti-VEGF treatment may lead clinicians to hold off anti-VEGF intervention in borderline treatment-requiring cases with posterior disease, for example, posterior zone II stage 2 with plus disease (UK ROP guideline[19]). As part of this study, we aimed to quantify and compare the rate of retinal vascularization before and after intravitreal anti-VEGF treatment for type 1 ROP.

METHODS

• **DATA COLLECTION AND STUDY ELIGIBILITY CRITERIA:** This study was conducted as an internal retrospective clinical audit approved by the Oxford University Hospitals Integrated Governance System (Oxford University Hospitals clinical audit approval no. 9080). Because of the retrospective and anonymous nature of this audit, informed consent was waived by the ethics committee.

The ROP database at the Oxford University Hospitals NHS Foundation Trust (a level 3 neonatal care unit, John Radcliffe Hospital, Oxford, UK) was searched retrospectively from May 2019 to February 2024 to identify all infants that underwent ROP screening in accordance with UK guidelines[19] with known outcomes and who had at least three 200° UWF retinal images (Optos California) captured at least 1 week apart. The ROP outcomes were classified into 3 clinical categories:

- Group A (no ROP): eyes that were recorded as having full or zone 3 retinal vascularization without developing any ROP and discharged from ROP screening;
- Group B (ROP not requiring treatment): eyes that had complete regression of ROP without reaching treatment threshold (ie, type 2 ROP);
- Group C (ROP requiring treatment): eyes with type 1 ROP that required treatment for ROP (either anti-VEGF therapy or laser).

Infants without definitive ROP outcomes (eg, infants that were transferred to other units or passed away) and those with other significant ocular comorbidity were excluded from the analysis. Eyes that did not have serial UWF imaging of sufficient quality to measure the extent of temporal retinal vascularization were also excluded.

The data set was used for the following 2 major analyses:

Analysis 1: Retinal vascularization rates as a predictor of type 1 ROP. To develop our machine learning model for predicting type 1 ROP, we excluded retinal images obtained after any ROP treatment or after 40 weeks' PMA to avoid bias, as fewer scans beyond 40 weeks' PMA would be associated with infants who do not develop any ROP.[20] Infants that started ROP screening from May 2019 up to the end of March 2023 were used to train the ROP prediction model. Infants not included in model training, who started screening from April 2023 to February 2024, were used as an independent test set to validate the predictive model.

Analysis 2: Effects of anti-VEGF therapy on retinal vascularization. To determine the effect of anti-VEGF treatment on the rate of retinal vascularization, we included all eyes with type 1 ROP with at least 2 UWF images captured before and 2 images after intravitreal injection of bevacizumab (0.16 mg in 0.025 mL). This ultra-low-dose bevacizumab is the clinical standard at

Oxford University Hospitals NHS Foundation Trust.[21] For this analysis, UWF images captured after 40 weeks' PMA were included to assess the long-term effects of anti-VEGF therapy on retinal vascularization.

Alongside the UWF retinal images, the following information were also collected for each infant: gestational age in weeks at birth (GA), birthweight (BW), ROP outcome based on International Classification of ROP,[10] PMA at each ROP screening time point, and PMA at the time of anti-VEGF injection (if applicable). PMA was defined as gestational age plus postnatal age.

• **UWF RETINAL IMAGE ANALYSIS:** All UWF retinal images used for analysis were captured using the same camera (Optos California). For each UWF retinal image, the advancement of temporal vascular front was measured as the ratio between the distance from the optic disc center to the temporal vascular front and that from the optic disc center to the fovea along a straight line that bisects the superior and inferior venous arcades. Identifying the fovea in preterm infants can be challenging because it is not as well defined owing to delayed or altered development in prematurity and ROP.[22,23]

For the purpose of consistent measurements across longitudinal UWF images, we defined the fovea as the point that bisects the widest distance between the superior and inferior venous arcades.[24] Retinal veins were chosen instead of arteries, as the arteries tend to become more tortuous in pre-plus or plus disease.[25] The red-free filter was used to provide improved contrast between vessels and the surrounding tissue to aid identification of vascular front and venous arcades.

To validate this approach, we performed fovea localization using the same method on confocal scanning laser ophthalmoscopy (cSLO) images accompanying Heidelberg Flex optical coherence tomography (OCT [Spectralis; Heidelberg Engineering, Germany]) in 13 eyes of 10 premature infants (Figure 1). Our protocol for Flex OCT was as previously described, with 768 A-scans and 73 B-scans over 55 × 30°.[26] The location of "presumed" fovea on the cSLO image was compared with the "actual" anatomical fovea as identified on the corresponding OCT. This showed a mean discrepancy of only 0.4 mm (SD = 0.36) between the presumed and actual fovea locations (Supplementary Table S1), thus validating our method for consistently identifying the fovea on UWF images.

The disc-to-fovea distance (D-F) was chosen as the reference unit of distance measurement so that subsequent disc-to-temporal vascular front distance measurements could be expressed as a ratio to D-F. This is consistent with the methodology used in previous studies.[27,28] In addition, De Silva and colleagues[29] demonstrated that longitudinal D-F measurements did not change significantly over 9 weeks in preterm and full-term infants. This normalization helps to eliminate the effects of small changes in image magnification or angle and axial length growth on calliper measurements taken from images of the same eye at different time points (Supplementary Figure S1, A). Using this method, temporal vascularization was observed to progress in a linear fashion in the untreated eyes of premature infants (Supplementary Figure S1, B).

It should be noted that although all eyes grow in size between 32 and 52 weeks' gestation (approximately 0.15 mm/wk, as described by Cook and colleagues[30]), the difference in the rate of axial length increase between normal and stage 1-3 ROP eyes is minimal and, importantly, all eyes follow linear growth trajectories over the period in question. The other practical benefit of using D-F distance as the reference unit is to allow inference of vascularization to the edge of zone I, because the diameter of zone I is defined as twice the distance from the fovea to the disc center (ie, 2 × D-F) (Supplementary Figure S1, B). The location of the temporal vascular front was measured until the posterior end of the vessel. However, if a vascular ridge was present, the location of the vascular front was defined as the center (or peak) of the ridge.

All distance measurements were made using the calliper tool within OptosAdvance (Optos plc.) with in-built peripheral retinal curvature correction that assumes the axial length to be 24 mm.[31-33] Therefore, we validated the use of the calliper tool in premature infants (who have axial lengths generally less than 24 mm) by looking at the disc-to-temporal vascular front distance / disc-to-fovea distance (DT/DF) ratios in untreated eyes where the vessels grew more peripheral and found no deviation in TVR that would have been expected if distance measurements became more distorted toward the periphery (Supplementary Figure S1, B).

These measurements were reviewed twice by investigator E.C. and reviewed by a second independent investigator (R.P.) to assess interrater correlation and achieve a consensus. Measurements of the disc-to-temporal vascular front were regressed against PMA (in weeks) at the time of imaging and the gradient of the line of best fit taken as the temporal vascularization rate (TVR) for an individual eye.

• **STATISTICAL ANALYSIS:** Statistical analysis was conducted using the programming software R (v4.2.1). Linear mixed effect modeling was used to account for repeated measures using the lme4 package.[34] Model performance and diagnostics were carried out using the performance package,[35] and effect size analysis for the linear mixed effects model was performed using the simr package.[36]

Temporal vascularization rate (TVR) for each eye was calculated using a linear regression slope analysis of the advancement of temporal vascular front vs PMA at imaging. As part of our preliminary work, the disc-to-nasal vascular front was also measured in a similar manner to disc-to-temporal vascular front in eyes that had UWF images that captured nasal peripheral retina on more than 1 occasion

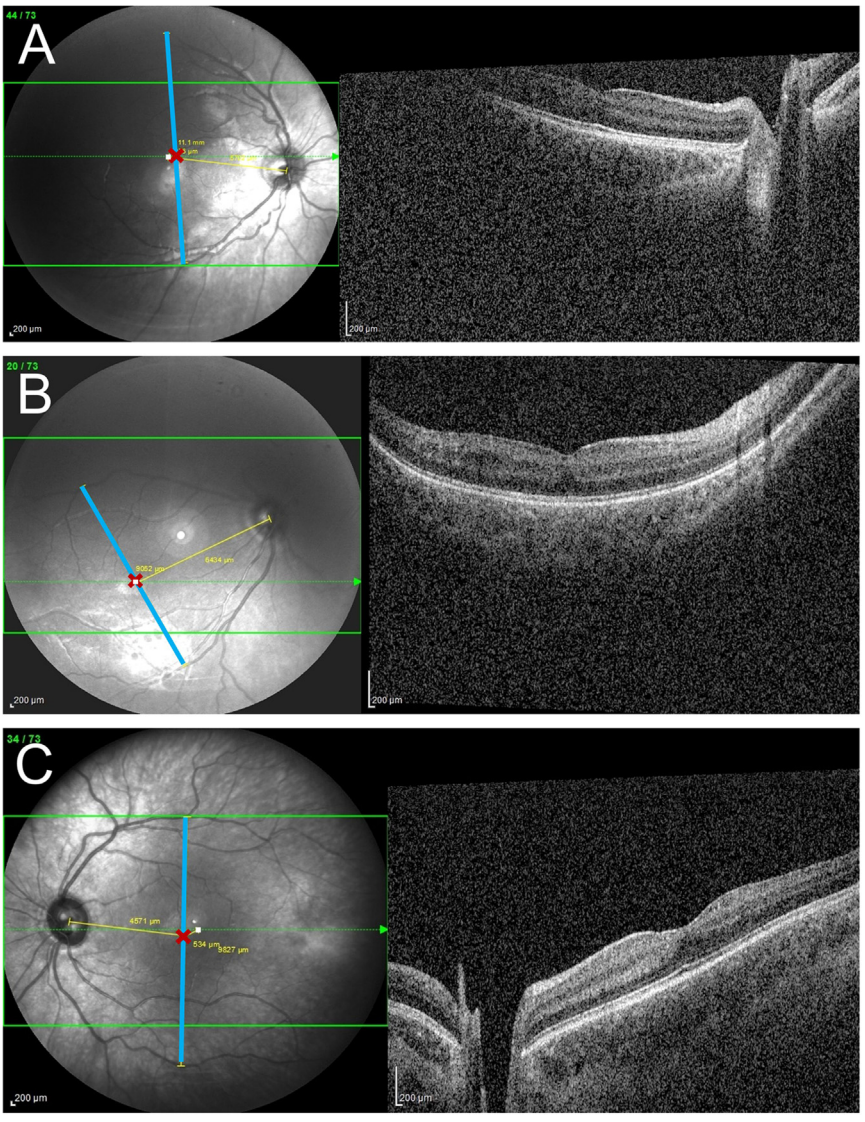

FIGURE 1. Validation of method for fovea localization in premature infants using Flex OCT. "Presumed" fovea (red cross) was defined on the Spectralis scanning laser ophthalmoscopy (SLO) images as the point that bisects the widest distance between the superior and inferior venous arcades (intersection between the yellow and blue lines). "Actual" (anatomical) fovea (white dot) was identified on the corresponding Spectralis Flex OCT and transferred to the SLO images using Heidelberg Eye Explorer (HEYEX) marker tool. A mean discrepancy of 0.40 mm (SD = 0.36) was achieved across 13 eyes of 10 premature infants imaged. Three representative examples are shown: A. Right eye of an infant born at 26 weeks with a discrepancy of 0.30 mm between presumed and actual fovea locations; B. Right eye of an infant born at 25 weeks with 0-mm discrepancy; C. Left eye of an infant born at 24 weeks with 0.53-mm discrepancy. OCT = optical coherence tomography.

(using D-F distance as the common unit). The advancement of nasal vascular front was found to correlate strongly with temporal vascular front with a correlation coefficient of 0.91 (Supplementary Figure S2). However, there were insufficient longitudinal data to calculate the nasal vascularization rate (NVR) for most eyes because of the technical challenge of consistently imaging the peripheral nasal retina. Therefore, all subsequent analyses used TVR as a surrogate measure of the overall rate of retinal vascularization for each eye.

To compare vascular growth rates between eyes that did not require treatment and those that did require treatment, group A and B eyes were combined to represent all those with no ROP or type 2 ROP (not requiring treatment). Group C included infants with type 1 ROP for which treatment is recommended per ICROP3 guidelines.[10] To detect differences in the rate of temporal retinal vascularization as a surrogate marker of overall vascularization rates (slopes) between these 2 groups, a linear mixed effect model with random slopes and random intercepts was fitted using both

eyes and patient ID as the nesting variables to account for similarities between right and left eyes in each patient and the repeated measures nature of the longitudinal data.

The fixed effect independent predictor variables investigated were the PMA, GA, BW, and ROP groups. The R package glmulti was used to compare all possible combinations of predictors along with their interactions.[37] Model comparisons were performed and evaluated using Akaike information criterion and Bayes information criterion to arrive at the best model to describe the independent variable of temporal vessel extent. The linear mixed effects analysis omnibus test was followed by a Tukey post hoc comparison of slopes.

Model assumptions were verified using visual normal distribution checks, q-q plot analysis, symmetry of histograms, and assessment of heteroscedasticity (Supplementary Figure S3). Where model assumptions were violated, such as in the comparison of TVR pre and post anti-VEGF treatment, robust linear mixed modeling was used. Robust models mitigate the effects of the outliers by applying a trimmed weighting to extreme outlier patients. An alternative Bayesian framework was also investigated; however the robust model fit was found to be superior, likely as a result of the presence of extreme outliers and the setting of vague priors because of a lack of existing knowledge in this novel domain.

Monte Carlo simulation adjusting effect sizes was implemented to determine the minimum effect size that could be reasonably detected at an alpha level of 0.05 and 90% power when compared to a null model.

• **DEVELOPMENT OF ROP CLASSIFICATION PREDICTION MODEL:** Gradient boosting is an ensemble machine learning technique that generates a large number of decision trees sequentially, each learning from the last, to accurately classify according to the observed predictors. We developed a model using gradient-boosting machine learning with the predictors, BW, GA, and TVR (slope coefficient of the temporal vascularization extent vs PMA), to predict whether an infant belongs to one of 2 groups: group AB (no treatment) or group C (ROP requiring treatment). We compared 3 models for prediction: one with TVR alone, one with BW and GA, and one model with all 3 predictors.

We chose to use a gradient boosting rather than random forest model because of the presence of nested data: the right and left eyes of each patient were included in the classification model. We used the package GPBoost, which combines linear mixed effects modeling and tree boosting to train the fixed effects and assign patient ID as the random effect to account for nested eyes.[38,39] GPBoost uses cross validation to tune the hyperparameters on the training data set.

Precision-recall curve (PRC) with area under the PRC (AUPRC) were calculated in addition to the receiver operating characteristic (ROC) curves and AUROC to assess each model from the training set. Both ROC and PR curves use sensitivity but the second axis differs: ROC uses a false positive rate (1 – specificity) whereas PRC uses precision defined as how many true positives out of all that have been predicted as positives. Although AUROC is more familiar to most, the AUPRC is a more suitable measure where there is class imbalance, particularly where there are far more negative cases than positive.[40,41] The moderate imbalance between the nontreatment group (n=48) and the ROP requiring treatment group (n=28) in our data set justifies the use of AUPRC over AUROC.

Bernoulli probit likelihood distribution was used for this binary classification training model, and the optimizer employed was Nesterov-accelerated gradient descent. The gradient-boosting predictive model was then tested using a fully independent validation set and assessed using balanced accuracy.

To establish whether TVR provides predictive information above that of BW and GA, we used a variable inflation factor analysis from the 'car' package[42] that assessed variable importance and the presence of collinearity. This assesses multicollinearity between the predictors (GA, BW, and TVR) by performing pairwise comparisons of every combination of predictors and analyzing each correlation coefficient obtained as a result.

For full code or information see Github link: github.com/amanasj/ROP-prediction-from-vascularisation-rates

RESULTS

• **DEMOGRAPHICS OF PATIENT GROUPS:** A total of 1204 infants underwent ROP screening during May 2019 to February 2024. Of these, 95 infants were included in the imaging analyses. Finally, 1109 infants were excluded mainly because of gradual transition from BIO to imaging-based ROP screening, transfer to other units, and insufficient number of UWF images.

Data from 76 infants (132 eyes) that started ROP screening from May 2019 to March 2023 were included in the training data set, and so used to investigate the rate of retinal vessel growth in infants with and without ROP requiring treatment and develop a predictive model. Note that the number of eyes to infants is not at 2:1 ratio due to exclusion of eyes with insufficient quality of UWF images for the delineation of temporal vascular front. Their mean GA was 26.0 (SD ±2.0) weeks and mean BW 815 (±264) g. Of the 76 infants, 22 infants (33 eyes) who did not develop any ROP were assigned to group A; 28 infants (49 eyes) who had type 2 ROP were assigned to group B; and 28 infants (50 eyes) with type 1 ROP requiring treatment were assigned to group C. Representative UWF images for groups A, B. and C are shown in Figure 2, A.

Patients in group A and group B were subsequently merged into a combined group AB, which represents all infants who did not require ROP treatment. Group AB consisted of 82 eyes from 48 infants. There is a discrepancy of 2

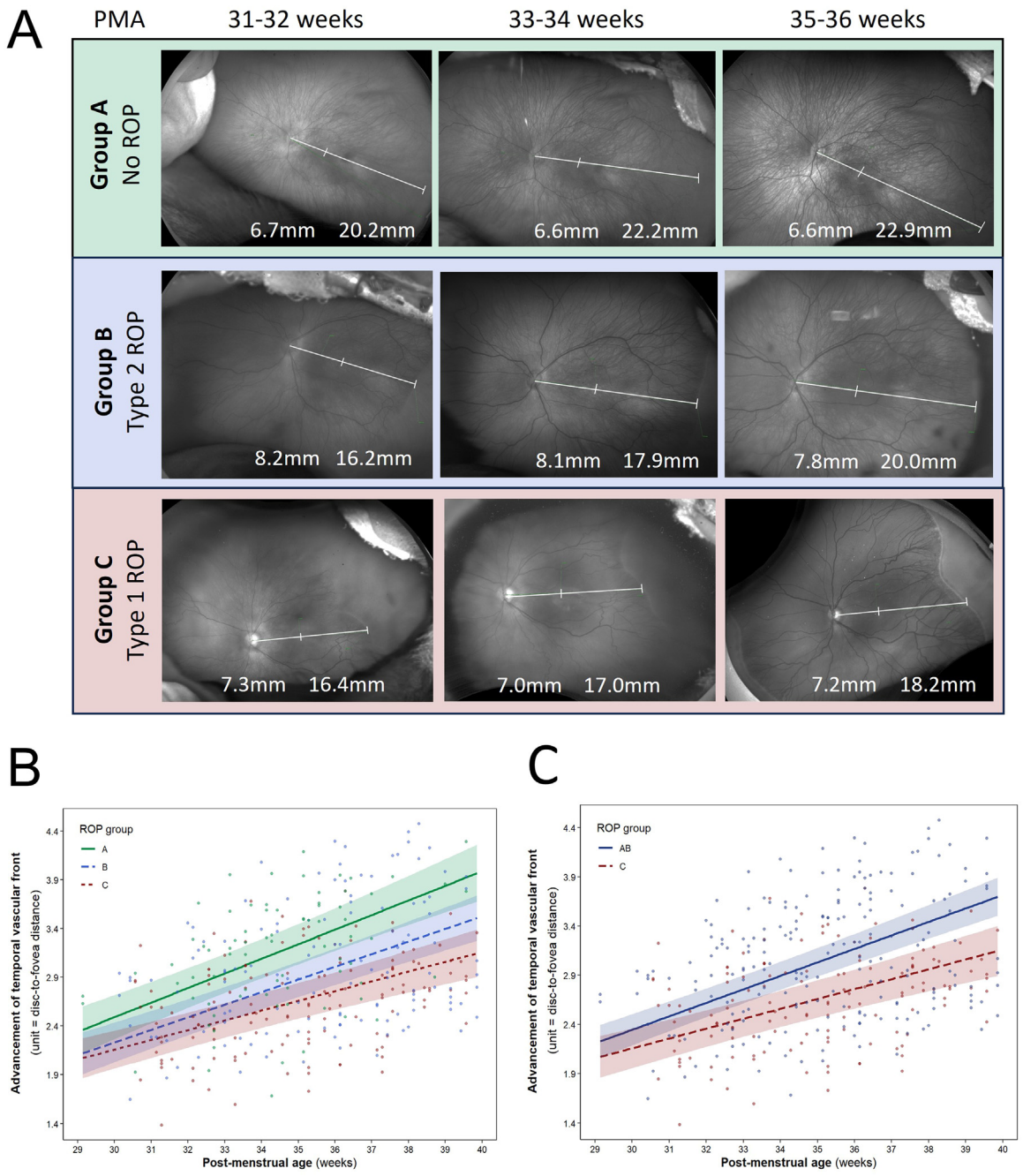

FIGURE 2. Correlation between temporal retinal vascularization rate (TVR) and ROP occurrence. A. Representative red-free UWF image series from consecutive ROP screening visits of eyes categorized as group A (no ROP at any time point), group B (type 2 ROP), and group C (type 1 ROP). For each image, measurements (mm) of the distance from disc center to fovea (*x*) and disc center to temporal vascular front (y) are taken along a straight line that bisects the widest distance between the superior and inferior venous arcades. This enables expression of the extent of advancement of temporal vascularization at each time point as a ratio (*x*/y). B. Comparison of advancement in temporal vascular front relative to postmenstrual age (weeks) between groups A (green), group B (blue), and group C (red). The slope represents the temporal vascularization rate (TVR), which serves as a surrogate marker for the rate of retinal vascularization for each group. Error bars represent 95% CI calculated at the "within subject" level using the linear mixed model. C. Comparison of advancement in temporal vascular front relative to postmenstrual age between the combined group AB (no ROP treatment required, dark blue) and group C (ROP requiring treatment, red). Mean TVR (slope) of group AB eyes is significantly greater than group C eyes ($P = .04$). ROP = retinopathy of prematurity.

TABLE 1. Demographics for Infants in Training and Test Groups.

Characteristic	Training Set (n=76 Infants)	Test Set (n = 19 Infants)
GA, wk, mean ± SD	26.0 ± 2.0	26.4 ± 1.5
BW, g, mean ± SD	815 ± 264	803 ± 240
Infants with type 1 ROP, n (%)	28 (37)	5 (26)

BW = birthweight, GA = gestational age, ROP = retinopathy of prematurity.

infants in the combined group, as these infants had one eye in group A and the other eye in group B. No infant in group AB received any anti-VEGF treatment or laser during the study.

The predictive model was tested using a fully independent test set containing data from 19 infants (32 eyes) that underwent ROP screening from April 2023 to February 2024 with all inclusion criteria fulfilled. Their mean GA was 26.4 (SD ±1.5) weeks and mean BW 803 (±240) g. Among these, 14 infants (24 eyes) did not require any treatment for ROP (group AB) whereas 5 infants (8 eyes) required treatment for ROP (group C). The demographics of training and test data sets are summarized in Table 1.

- **ANALYSIS 1:**

Slow rate of advancement of temporal retinal vascular front is associated with ROP

Across the training cohort, we found a trend for the TVR to decrease with increasing severity of ROP: the mean (±SEM) TVR for group A eyes was 0.15 (±0.017) disc-to-fovea distance per week (D-F/wk), group B (ROP not requiring treatment) was 0.13 (±0.013) D-F/wk, and group C (ROP requiring treatment) 0.10 (±0.013) D-F/wk (Figure 2, B). Omnibus analysis of variance revealed significant differences in TVR ($P = .049$); however, post hoc testing with Tukey correction revealed no significant pairwise differences in TVR between group A and B ($P = .60$), between group B and C ($P = .26$), or between group A and C ($P = .059$).

Given the clinical importance of distinguishing treatment-requiring vs non–treatment-requiring ROP and the somewhat subjective distinction between no ROP and stage 1 ROP, we merged group A and B eyes into a combined group AB (ie, all eyes that did not require any therapeutic intervention) and compared this group with group C (Figure 2, C). In this case, the TVR of group C was significantly slower (by 29%) than the TVR of group AB ($P = .04$, TVR of group AB = 0.14±0.01 D-F/wk, group C = 0.10±0.014 D-F/wk).

Vascularization rate as a predictor of type 1 ROP

Given the significant difference in TVR between infants with and without ROP treatment, we hypothesized that TVR, calculated from at least 2 successive ROP screening visits, could be used as an independent predictor of type 1 ROP, over and above decisions based on GA and BW alone. A machine learning predictive model was developed using the training data set, comparing 3 models incorporating (1) TVR only, (2) BW+GA, or (3) TVR+BW+GA as predictors (Figure 3, A). The models were then tested using a fully independent test set as detailed above.

Although the combined predictive model (TVR+BW+GA) showed the best performance with an area under the precision recall curve (AUPRC) of 0.84 (Figure 3, A) (AUROC 0.90, Supplementary Figure S4), the model with TVR alone still performed well with an AUPRC 0.6 (AUROC 0.75). In the combined model, the model attributed percentage importance to each predictor for classifying type 1 ROP as 63% to BW, 32% to GA, and 5% to TVR (Figure 3, B). Moreover, variable inflation factor analysis confirmed that TVR independently contributes to the predictive accuracy of the model with minimal collinearity with BW ($r = 0.16$) or GA ($r = 0.10$). This is in contrast to moderate or high collinearity between BW and GA ($r = 0.70$). The VIF analysis also showed that any multicollinearity between PMA contained in the TVR calculation and GA was small to moderate.

In the independent test set, the combined model correctly predicted the outcomes of 30/32 eyes based on BW, GA, and TVR (Figure 3, A, and Table 2). The balanced accuracy on the test data was 95.8%. The incorrect predictions were both eyes of patient Test15, which were predicted as belonging to group C when the actual outcome was group AB.

- **ANALYSIS 2:**

Effects of anti-VEGF therapy on retinal vascularization rate

To quantify the effect of anti-VEGF therapy on retinal vascularization rate, we compared the TVR before and after treatment. Within our data set, there were 37 eyes (from 20 infants) that received intravitreal bevacizumab injection (0.16 mg in 0.025 mL per eye) for ROP as well as having at least 2 UWF imaging time points before and 2 after the treatment (Figure 4, A). Their mean (±SD) GA at birth was 24.2 (±0.9) weeks and BW 599 (±124) g. The mean follow-up length after anti-VEGF injection was 7.7 (±7.9) weeks, with a minimum follow-up of 2 days and a maximum follow-up of 43 weeks.

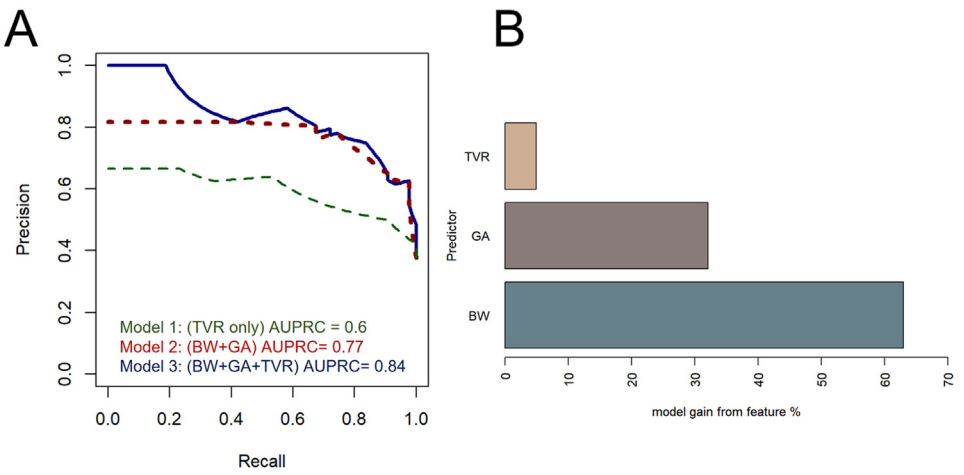

FIGURE 3. Temporal retinal vascularization rate predicts type 1 ROP. A. Comparison of the precision-recall curves for 3 different prediction models. Dark-blue solid line represents model with predictors as birthweight (BW), gestational age (GA), and temporal vascularization rate (TVR) that was used for further prediction. B. Feature importance showing relative contributions of each predictor for the classification between treatment vs no treatment groups. AUPRC = area under the precision-recall curve, ROP = retinopathy of prematurity.

During the study period, only 1 eye of 1 infant (number 8 in Figure 4, A) within this group was retreated with a second injection of intravitreal ranibizumab (0.2 mg) 1 week after primary bilateral bevacizumab treatment because of the lack of regression seen. We suspect this may have been due to drug reflux during the primary injection. After the study period, 3 infants received bilateral laser for reactivation of ROP (numbers 1, 10, and 16 in Figure 4, A) at 43.6 weeks', 41.7 weeks', and 70.9 weeks' PMA, respectively.

Linear mixed model analysis showed no significant difference in TVR before and after anti-VEGF injection for both the right eyes ($P = .60$) and the left eyes ($P = .71$). Patients individually showed a mixture of changes (both increases and decreases) in TVR posttreatment, but collectively this was not statistically significant (Figure 4, B). Post hoc effect size analysis using Monte Carlo simulation demonstrated that there was sufficient sample size to detect a 3.3% (95% CI: 2.8-3.5) change in TVR after treatment (at alpha = 0.05 and power = 90%). Therefore, we conclude that anti-VEGF therapy does not significantly alter the rate of temporal retinal vascularization.

DISCUSSION

It is commonly observed during ROP screening that retinal vascularization of zone II is complete at 34 weeks' PMA in the low-risk infants, whereas vascularization has only reached the posterior zone II in the high-risk infants for ROP at the same PMA.[11] This delayed retinal vascularization may be a common end result of various major ROP risk factors. In this study, we hypothesized that direct quantification of the rate of retinal vascularization through longitudinal UWF imaging could enable early prediction of type 1 ROP. Our results demonstrate that the slow rate of temporal vascularization is correlated with ROP severity and can be used, along with BW and GA, to predict eyes that develop type 1 ROP with 96% accuracy. The results demonstrate the benefit of using the retinal vascularization rate derived from UWF imaging-based ROP screening, highlighting its ability to provide novel quantitative insights into disease progression and treatment response early in the screening/monitoring process.

One of the considerations motivating us to use the disc-to-fovea (D-F) distance as a reference unit is because it is featured within the definition of zone I, such that 2 × D-F would approximate the edge of zone I (as shown by dotted lines in Figure 4, A). Consequently, the extent of retinal vascularization expressed as a multiple of D-F would be practically meaningful to a clinical assessor. Although we routinely captured Optomap images with the eyes in primary position and at a set distance from the camera, some variability in distance measurements due to fluctuations in imaging angle and centration are unavoidable. However, by calculating and comparing the rate (rather than absolute extent) of temporal vascularization (TVR) using the gradient of regression lines across several time points, we tried to minimize the effects of measurement errors and variability at individual time points (Figure 2, B and C).

Although UWF imaging of the temporal retinal vasculature is most consistently captured with the "flying baby" imaging technique, we also evaluated the advancement of nasal vascular front where data were available as part of an initial exploratory study and found this to strongly correlate with advancement of temporal vascular front (Supplemental Figure S1). On this basis, TVR was chosen

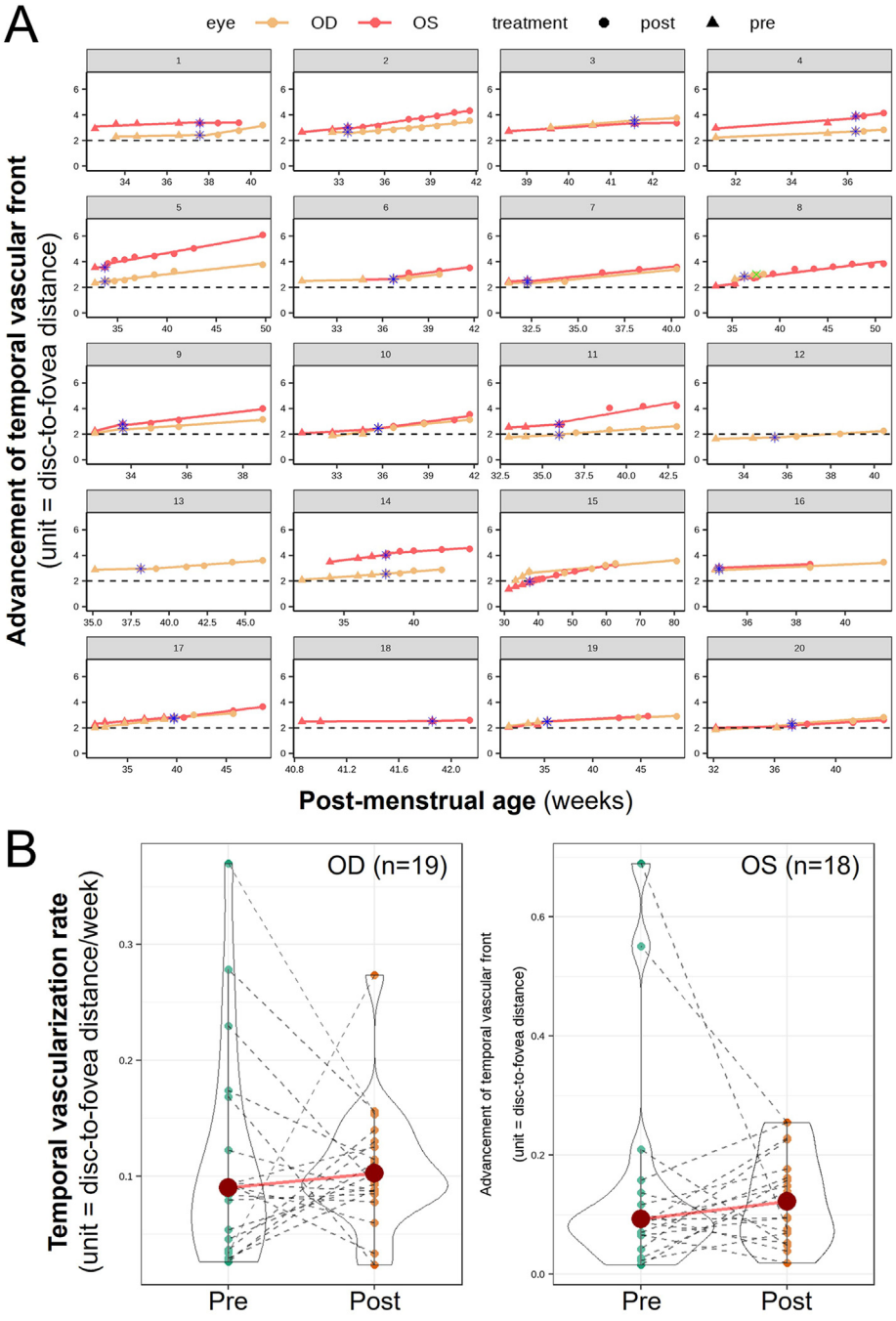

FIGURE 4. No significant difference between the temporal retinal vascularization rate (TVR) before and after anti-VEGF therapy for ROP. A. Comparison of advancement of temporal vascular front before and after bevacizumab (0.16 mg) injection in 20 infants (37 eyes). Each plot is from a different infant. Each triangle (pretreatment) or circle (posttreatment) denotes an ultra-widefield (Optomap) imaging time point. The solid colored line is the regression slope. The blue asterisk denotes the postmenstrual age at which intravitreal injection of bevacizumab 0.16 mg was given. Green cross for infant number 8 denotes retreatment with an injection of intravitreal ranibizumab (0.2 mg) 1 week after primary bilateral bevacizumab treatment due to lack of regression seen. Slope to the left of the asterisk is the TVR pretreatment and slope to the right of the blue asterisk is the TVR posttreatment. Dotted line at y = 2 where the ratio of disc-to-temporal vascular front distance to disc-to-fovea distance is 2, corresponds to the dividing line between zone I and zone II. B. Violin plots comparing temporal vascularization rate before and after bevacizumab (0.16 mg) injection for 19 right eyes and 18 left eyes. Each dotted line represents a single eye with temporal vascularization before (green dot) and after treatment (orange dot). The red circle represents the mean temporal vascularization rate (disc-to-fovea distance [D-F]/wk). anti-VEGF = anti–vascular endothelial growth factor, OD = right eye, OS = left eye, ROP = retinopathy of prematurity.

TABLE 2. Predicting Type 1 ROP in a Test Data Set Using a Gradient-Boosting Model.

ID	Eye	GA (weeks)	BW (g)	TVR (D-F/wk)	Actual ROP group	Model prediction (TVR+GA+BW)
Test1	OS	26.86	1,080	0.059	AB	AB
Test1	OD	26.86	1,080	0.162	AB	AB
Test2	OS	26.86	1,025	0.150	AB	AB
Test2	OD	26.86	1,025	0.114	AB	AB
Test3	OD	27.29	1,085	0.099	AB	AB
Test4	OS	27.43	680	0.148	AB	AB
Test4	OD	27.43	680	0.414	AB	AB
Test5	OS	27.71	1,185	0.105	AB	AB
Test5	OD	27.71	1,185	0.099	AB	AB
Test6	OD	26.29	455	0.030	C	C
Test7	OS	24.00	390	0.137	C	C
Test7	OD	24.00	390	0.068	C	C
Test8	OS	26.29	725	0.092	AB	AB
Test8	OD	26.29	725	0.078	AB	AB
Test9	OD	26.14	540	0.130	AB	AB
Test10	OS	25.57	755	0.083	C	C
Test10	OD	25.57	755	0.054	C	C
Test11	OS	26.14	980	0.070	AB	AB
Test11	OD	26.14	980	0.080	AB	AB
Test12	OS	28.29	1,090	0.281	AB	AB
Test12	OD	28.29	1,090	0.685	AB	AB
Test13	OD	29.29	1,035	0.152	AB	AB
Test14	OD	23.71	540	0.046	C	C
Test15	OS	24.71	650	0.102	AB	C
Test15	OD	24.71	650	0.131	AB	C
Test16	OS	28.29	880	0.004	AB	AB
Test16	OD	28.29	880	0.058	AB	AB
Test17	OS	25.71	875	0.210	AB	AB
Test17	OD	25.71	875	0.139	AB	AB
Test18	OS	27.43	690	0.365	AB	AB
Test19	OS	24.14	590	0.066	C	C
Test19	OD	24.14	590	0.129	C	C

D-F= disc-to-fovea distance, BW = birthweight, GA = gestational age, ROP = retinopathy of prematurity, TVR = temporal vascularisation rate.

Test15 highlights a case of discrepancy between model prediction and actual ROP categorisation.

Group AB: no ROP + type 2 ROP (non–treatment-requiring group). Group C: type 1 ROP (treatment-requiring ROP group).

as a clinically convenient surrogate marker for overall retinal vascularization.

Our findings demonstrate a significantly (29%) slower rate of retinal vascularization in eyes that develop type 1 ROP (group C) compared with eyes with no ROP or type 2 ROP (group AB). This is consistent with previous reports evaluating the rate of retinal vascularization based on indirect ophthalmoscopy,[14] timing of vascular front reaching zone II,[11] and contact wide-field imaging using RetCam.[13] The major advantage of using UWF imaging is that it allows rapid, noncontact, and longitudinal monitoring of retinal vascularization from birth to mid- or late infancy (up to the age of 50 weeks in our cohort), consistently capturing the temporal vascular front up to anterior zone II (without the need to collage images).

The risk factors contributing to delayed retinal vascularization in premature infants, and therefore increased risk of severe ROP, include oxygen supplementation or fluctuation,[43-45] mechanical ventilation or CPAP,[15,46-48] and poor postnatal weight gain.[49] It has been proposed to result from a drop in serum insulin-like growth factor (IGF-1) level due to loss of maternal supply and poor endogenous production during extreme prematurity. Because IGF-1 has a permissive role in VEGF signaling, low serum IGF-1 prevents retinal vessel growth in response to VEGF produced by the ischemic avascular retina. As the infant grows bigger, endogenous IGF-1 production eventually catches up, thus permitting a rebound in VEGF signaling that drives the proliferative phase of ROP.[50] Based on this model, postnatal weight gain has been proposed

and shown as a biomarker for serum IGF-1 level and ROP risk.[49]

Our UWF imaging-based method provides the most direct and consistent measurements of retinal vascularization rate as of this writing, which could be calculated from the earliest ROP screening visits (eg, <32 weeks' PMA) in extreme premature infants to facilitate early prediction and intervention to reduce the risk of developing type 1 ROP.

Our gradient-boosting machine learning model, incorporating TVR along with BW and GA, was able to predict those eyes requiring ROP treatment with 96% balanced accuracy, 100% sensitivity, 92% specificity, negative predictive value of 80%, and positive predictive value of 100%, within a limited sample size validation test data set. Although the prediction power of BW+GA and BW+GA+TVR models appear similar from the AUROC values 0.89 vs 0.90 (Supplementary Figure S4), the more appropriate AUPRC values that consider the moderate class imbalance between the nontreatment group and the ROP requiring treatment group in our sample were 0.77 vs 0.84, which demonstrates an improvement following the addition of TVR (Figure 3, A). Furthermore, the predictive power of BW+GA alone may be overestimated because of the limited sample size and particular nature of this cohort. A previous study obtained an AUROC for BW+GA of 0.808.[51]

The addition of TVR to BW+GA for type 1 ROP prediction is also clinically meaningful as it improved the specificity of prediction from 87.5% with BW+GA alone to 92%, thus reducing false positive predictions. For instance, our combined TVR+BW+GA model correctly predicted infant Test 9 as not requiring treatment (group AB), whereas the BW+GA model incorrectly predicted this infant as ROP requiring treatment, likely because of the infant's BW (540 g) and GA (26.1 weeks) being below average for the validation set (803 g and 26.4 weeks, respectively). Furthermore, infant Test10 is an example where, despite both BW (755 g) and GA (25.6 weeks) being higher than Test15, the combined model overrode this information and accurately assigned group C based on low TVR (0.08 and 0.05) in both eyes.

The variable inflation factor analysis also shows that TVR acts as an independent prediction factor over BW and GA (Figure 3, B). Taken together, these findings suggest that TVR could provide added clinical value in ambiguous cases where it refines the typical correlation between BW/GA and ROP. Future work to identify clinical factors that modulate the rate of retinal vascularization would also be beneficial for identifying novel therapeutic strategies to prevent ROP.

Across a cohort of 37 eyes (of 20 infants) that received intravitreal injection of bevacizumab (0.16 mg) for type 1 ROP between 32.5 and 39 weeks' PMA, we found that anti-VEGF treatment does not significantly alter the rate of physiological retinal vascularization. Although there were individual examples of decreased TVR post anti-VEGF treatment, the overall trend of the cohort was in fact a slight but nonsignificant increase in TVR, which was seen in both left eyes and right eyes (Figure 4, B).

Sauer and colleagues[52] recently reported that bevacizumab (0.25 mg) may increase vessel extension into the PAR within 2-4 weeks of treatment. The difference in the findings from Sauer and colleagues[52] and this study may be due to a number of factors. These include difference in bevacizumab dose (0.25 mg vs 0.16 mg), difference in the duration of posttreatment follow-up (2-4 weeks vs mean 7.7 weeks ± 7.9 SD in this study), which relates to the different imaging modalities used (RetCam vs Optomap). Moreover, we compared the rate of temporal vascularization (TVR) posttreatment to pretreatment for each eye, whereas Sauer and colleagues.[52] compared the absolute extent of temporal vascularization in treated eyes against untreated eyes from GA- and BW-matched controls. These differences in methodology mean that findings from the 2 studies are not directly comparable.

Our post hoc power analysis suggests that our data set should enable us to detect a 3.3% change in TVR at 90% power; thus, it is possible that a less than 3.3% change would not have been detected. Nevertheless, both studies indicate that low-dose or ultra-low-dose bevacizumab does not slow or halt physiological retinal vascularization. Taken together, these findings suggest that low-dose intravitreally administered bevacizumab may be sufficient to inhibit pathologic intravitreal neovascularization without significantly interfering with physiological intraretinal vascularization, possibly because of difference in drug concentration across the retina or target VEGF receptors. Further studies are needed to study the effects of higher doses or alternative anti-VEGF agents on retinal vascularization.

Of note, the infants who did show reductions in TVR appear to be ones with unusually high pretreatment vascularization rates. Although there may be some lag in change of vascularization rate after treatment, our follow-up period (mean 7.7 weeks ± 7.9 SD) extended far beyond the half-life of intravitreal bevacizumab (shown to be 5-7 days),[53,54] including 2 infants observed for over 16 weeks without signs of reduced vascularization rate. Furthermore, posttreatment TVR also may be affected by the persistence of ROP. Among the 20 bevacizumab-treated infants in analysis 2, there were 2 infants with incomplete regression of ROP during the study period (infants no. 15 and 17 in Figure 4, A). After the study period, 3 other infants developed ROP reactivation requiring laser treatment (nos. 1, 10, and 16 in Figure 4, A). Future work is needed to identify what may determine the rate of temporal vascularization and whether the heterogeneity in this characteristic may influence response to anti-VEGF treatment and rate of reactivation.

These intriguing findings challenge the assumption that anti-VEGF treatment slows physiological retinal vascularization or causes vascular arrest, thus leading to the development of PAR.[10,55,56] This perceived disadvantage of anti-

VEGF may encourage treating clinicians to delay intervention in eyes that are borderline for treatment (eg, posterior zone II, stage 2 with plus disease or stage 3 with pre-plus disease). Our findings provide novel insights on retinal vascularization in premature infants with 3 main implications.

First, the results suggest that ultra-low-dose (0.16 mg) intravitreal bevacizumab may selectively target pathologic extraretinal neovascularization without significant interference of physiological intraretinal vascularization. Second, the development of PAR is likely a result of slower rate of retinal vascularization from birth in some extreme premature infants (as evidenced by our finding of slower TVR in eyes with more severe ROP), rather than a consequence of anti-VEGF therapy.

PAR may have been previously underrecognized with laser photocoagulation to avascular peripheral retina but has become more apparent with increasing use of anti-VEGF as the primary treatment modality. This has significant clinical implications for the etiology of PAR and the timing of anti-VEGF treatment, suggesting the need to explore potential benefits of earlier intervention to suppress pathologic neovascularization (eg, at stage 2 with popcorn lesions or in cases of retinal edge hemorrhage), which could prevent subsequent complications of more advanced ROP (eg, fibrosis and vessel dragging that may complicate regressed stage 3 disease).

One such approach could target VEGF receptor 2 (VEGFR2) signaling in retinal endothelial cells (ECs). Experimentally it has been shown that selective knockdown of VEGFR2 signaling in rodent retinal endothelial cells could inhibit intravitreal neovascularization by preventing disordered division of retinal ECs during angiogenesis while facilitating physiological retinal vascularization longitudinally.[57-59] However, current intravitreal anti-VEGF agents may not be sufficiently selective to only target VEGFR2 signaling in retinal ECs.

This is a single-center retrospective cohort study. Eyes with poor UWF image quality (that precluded accurate measurement of vascular front) were excluded, which could potentially introduce selection bias into the data set. As a result, the gradient-boosting predictive model was trained and tested on relatively small data sets. To further refine the prediction model, it would benefit from larger training data sets from multiple centers with prospective data collection. Our protocol for UWF imaging-based ROP screening has been successfully adopted at several neighboring ROP screening units, which would help future improvement and validation of the model.

In summary, UWF imaging-based ROP screening enables continuous monitoring of retinal vascularization rate, which provides an early biomarker for treatment-requiring ROP. The rate of retinal vascularization does not appear to be affected by 0.16 mg intravitreal bevacizumab treatment, which has significant implications for the etiology of PAR and optimal timing of anti-VEGF treatment for ROP. Future work will explore the effects of oxygenation and comorbidities on the rate of retinal vascularization at different PMAs.

Funding/Support: Kanmin Xue has received funding from the Wellcome Trust (216593/Z/19/Z) and National Institute for Health and Care Research (NIHR) Oxford Biomedical Research Centre (BRC). Caroline Hartley is funded by the Wellcome Trust (213486/Z/18/Z). Financial Disclosures: The authors indicate no financial support or conflicts of interest. All authors attest that they meet the current ICMJE criteria for authorship.

REFERENCES

1. Solebo AL, Teoh L, Rahi J. Epidemiology of blindness in children. *Arch Dis Child*. 2017;102(9):853–857. doi:10.1136/ARCHDISCHILD-2016-310532.
2. Ashton N. Pathological basis of retrolental fibroplasia. *Br J Ophthalmol*. 1954;38(7):385–396. doi:10.1136/BJO.38.7.385.
3. Hartnett ME, Penn JS. Mechanisms and management of retinopathy of prematurity. *N Engl J Med*. 2012;367(26):2515–2526. doi:10.1056/NEJMRA1208129.
4. Patz A, Hoeck LE, De La, Cruz E. Studies on the effect of high oxygen administration in retrolental fibroplasia. I. Nursery observations. *Am J Ophthalmol*. 1952;35(9):1248–1253. doi:10.1016/0002-9394(52)91140-9.
5. Blencowe H, Lawn JE, Vazquez T, Fielder A, Gilbert C. Preterm-associated visual impairment and estimates of retinopathy of prematurity at regional and global levels for 2010. *Pediatr Res*. 2013;74(Suppl 1):35–49. doi:10.1038/PR.2013.205.
6. Bhatnagar A, Skrehot HC, Bhatt A, Herce H, Weng CY. Epidemiology of retinopathy of prematurity in the US from 2003 to 2019. *JAMA Ophthalmol*. 2023;141(5):479–485. doi:10.1001/JAMAOPHTHALMOL.2023.0809.
7. Royal College of Paediatrics and Child Health. *UK screening of Retinopathy of Prematurity Guideline*; March 2022.
8. Dammann O, Hartnett ME, Stahl A. Retinopathy of prematurity. *Dev Med Child Neurol*. 2023;65(5):625–631. doi:10.1111/DMCN.15468.
9. Hartnett ME. Pathophysiology of retinopathy of prematurity. *Annu Rev Vis Sci*. 2023;9:39–70. doi:10.1146/ANNUREV-VISION-093022-021420.
10. Chiang MF, Quinn GE, Fielder AR, et al. International Classification of Retinopathy of Prematurity, Third Edition. *Ophthalmology*. 2021;128(10):e51–e68. doi:10.1016/J.OPHTHA.2021.05.031.
11. Jang JH, Kim YC. Retinal vascular development in an immature retina at 33–34 weeks postmenstrual age predicts retinopathy of prematurity. *Scientific Reports 2020 10:1*. 2020;10(1):1–8. doi:10.1038/s41598-020-75151-0.
12. Kumar V, Surve A, Kumawat D, et al. Ultra-wide field retinal imaging: A wider clinical perspective. *Indian J Ophthalmol*. 2021;69(4):824–835. doi:10.4103/IJO.IJO_1403_20.

13. Padhi TR, Bhusal U, Padhy SK, et al. The retinal vascular growth rate in babies with retinopathy of prematurity could indicate treatment need. *Indian J Ophthalmol*. 2022;70(4):1270–1277. doi:10.4103/IJO.IJO_1484_21.
14. Solans Pérez de Larraya AM, Ortega Molina JM, Fernández JU, et al. Retinal vascular speed <0.5 disc diameter per week as an early sign of retinopathy of prematurity requiring treatment. *Eur J Ophthalmol*. 2018;28(4):441–445. doi:10.1177/1120672118761328.
15. Solans Pérez De Larraya AM, Ortega Molina JM, Uberos Fernández J, González Ramírez AR, Garcia Serrano JL. Speed of retinal vascularization in retinopathy of prematurity: risk and protective factors. *Biomed Res Int*. 2019;2019(1):2721578. doi:10.1155/2019/2721578.
16. Patel CK, Fung THM, Muqit MMK, et al. Non-contact ultra-widefield imaging of retinopathy of prematurity using the Optos dual wavelength scanning laser ophthalmoscope. *Eye*. 2013;27(5):589–596 *2013 27:5*. doi:10.1038/eye.2013.45.
17. Lepore D, Quinn GE, Molle F, et al. Follow-up to age 4 years of treatment of type 1 retinopathy of prematurity intravitreal bevacizumab injection versus laser: fluorescein angiographic findings. *Ophthalmology*. 2018;125(2):218–226. doi:10.1016/J.OPHTHA.2017.08.005.
18. Toy BC, Schachar IH, Tan GSW, Moshfeghi DM. Chronic vascular arrest as a predictor of bevacizumab treatment failure in retinopathy of prematurity. *Ophthalmology*. 2016;123(10):2166–2175. doi:10.1016/J.OPHTHA.2016.06.055.
19. Treating Retinopathy of Prematurity in the UK | The Royal College of Ophthalmologists. Accessed February 6, 2025. https://www.rcophth.ac.uk/resources-listing/uk-retinopathy-of-prematurity-guideline/
20. Pruett J, Ruland K, Donahue S. Validation of a published model to reduce burden of retinopathy of prematurity screening. *Am J Ophthalmol*. 2024;257:12–15. doi:10.1016/J.AJO.2023.09.004.
21. Hillier RJ, Connor AJ, Shafiq AE. Ultra-low-dose intravitreal bevacizumab for the treatment of retinopathy of prematurity: a case series. *Br J Ophthalmol*. 2018;102(2):260–264. doi:10.1136/BJOPHTHALMOL-2017-310408.
22. Akula JD, Arellano IA, Swanson EA, et al. The fovea in retinopathy of prematurity. *Invest Ophthalmol Vis Sci*. 2020;61(11) 28-28. doi:10.1167/IOVS.61.11.28.
23. Isenberg SJ. Macular development in the premature infant. *Am J Ophthalmol*. 1986;101(1):74–80. doi:10.1016/0002-9394(86)90467-8.
24. Wilson C, Theodorou M, Cocker KD, Fielder AR. The temporal retinal vessel angle and infants born preterm. *Br J Ophthalmol*. 2006;90(6):702–704. doi:10.1136/BJO.2005.085019.
25. An International Classification of Retinopathy of Prematurity. *Arch Ophthalmol*. 1984;102(8):1130–1134. doi:10.1001/ARCHOPHT.1984.01040030908011.
26. Purohit R, Rufai SR, Patel CK, et al. Feasibility of a portable optical coherence tomography system in children with craniosynostosis. *Eye (Lond)*. 2023;37(3):576–577. doi:10.1038/S41433-022-02205-0.
27. Lorenz B, Stieger K, Jäger M, et al. Retinal vascular development with 0.312 mg intravitreal bevacizumab to treat severe posterior retinopathy of prematurity: a longitudinal fluorescein angiographic study. *Retina*. 2017;37(1):97–111. doi:10.1097/IAE.0000000000001126.
28. Zhang X, Peng J, Yang Y, et al. Vascular development analysis: a study for tertiary anti-vascular endothelial growth factor therapy after second reactivation of retinopathy of prematurity. *Front Med (Lausanne)*. 2024;11:1421894. doi:10.3389/FMED.2024.1421894/BIBTEX.
29. De Silva DJ, Cocker KD, Lau G, Clay ST, Fielder AR, Moseley MJ. Optic disk size and optic disk-to-fovea distance in preterm and full-term infants. *Invest Ophthalmol Vis Sci*. 2006;47(11):4683–4686. doi:10.1167/IOVS.06-0152.
30. Cook A, White S, Batterbury M, Clark D. Ocular growth and refractive error development in premature infants with or without retinopathy of prematurity. *Invest Ophthalmol Vis Sci*. 2008;49(12):5199–5207. doi:10.1167/IOVS.06-0114.
31. Nagiel A, Lalane RA, Sadda SR, Schwartz SD. Ultra-widefield fundus imaging: a review of clinical applications and future trends. *Retina*. 2016;36(4):660–678. doi:10.1097/IAE.0000000000000937.
32. Sagong M, Van Hemert J, Olmos De Koo LC, Barnett C, Sadda SR. Assessment of accuracy and precision of quantification of ultra-widefield images. *Ophthalmology*. 2015;122(4):864–866. doi:10.1016/J.OPHTHA.2014.11.016.
33. Tan CS, Chew MC, Van Hemert J, Singer MA, Bell D, Sadda SR. Measuring the precise area of peripheral retinal non-perfusion using ultra-widefield imaging and its correlation with the ischaemic index. *Br J Ophthalmol*. 2016;100(2):235–239. doi:10.1136/BJOPHTHALMOL-2015-306652.
34. Bates D, Mächler M, Bolker BM, Walker SC. Fitting linear mixed-effects models using lme4. *J Stat Softw*. 2015;67(1):1–48. doi:10.18637/JSS.V067.I01.
35. Lüdecke D, Ben-Shachar MS, Patil I, Waggoner P, Makowski D. performance: an R package for assessment, comparison and testing of statistical models. *J Open Source Softw*. 2021;6(60):3139. doi:10.21105/JOSS.03139.
36. Green P, Macleod CJ. simr: an R package for power analysis of generalized linear mixed models by simulation. *Methods Ecol Evol*. 2016;7(4):493–498. doi:10.1111/2041-210X.12504.
37. Calcagno V. Model selection and multimodel inference made easy [R package glmulti version 1.0.8]. *CRAN: Contributed Packages*. 2020 Published online May 26. doi:10.32614/CRAN.PACKAGE.GLMULTI.
38. Sigrist F. Gradient and Newton boosting for classification and regression. *Expert Syst Appl*. 2021;167. doi:10.1016/j.eswa.2020.114080.
39. Sigrist F, Gyger T, Kuendig P. gpboost: combining tree-boosting with Gaussian process and mixed effects models. *CRAN: Contributed Packages*. 2021 Published online February 17. doi:10.32614/CRAN.PACKAGE.GPBOOST.
40. Davis J, Goadrich M. The relationship between precision-recall and ROC curves. *ACM Int Conf Proc Ser*. 2006;148:233–240. doi:10.1145/1143844.1143874.
41. Saito T, Rehmsmeier M. The precision-recall plot is more informative than the ROC plot when evaluating binary classifiers on imbalanced datasets. *PLoS One*. 2015;10(3):e0118432. doi:10.1371/JOURNAL.PONE.0118432.
42. Fox J, Weisberg S, Price B. Companion to applied regression [R package car version 3.1-3]. *CRAN: Contributed Packages*. 2024 Published online September 27. doi:10.32614/CRAN.PACKAGE.CAR.

43. Poppe JA, Fitzgibbon SP, Taal HR, et al. Early prediction of severe retinopathy of prematurity requiring laser treatment using physiological data. *Pediatr Res*. 2023;94(2):699–706. doi:10.1038/S41390-023-02504-6.
44. Hartnett ME, Lane RH. Effects of oxygen on the development and severity of retinopathy of prematurity. *J AAPOS*. 2013;17(3):229–234. doi:10.1016/J.JAAPOS.2012.12.155.
45. Rivera JC, Sapieha P, Joyal JS, et al. Understanding retinopathy of prematurity: update on pathogenesis. *Neonatology*. 2011;100(4):343–353. doi:10.1159/000330174.
46. Allegaert K, De Coen K, Devlieger H. Threshold retinopathy at threshold of viability: the EpiBel study. *Br J Ophthalmol*. 2004;88(2):239–242. doi:10.1136/BJO.2003.027474.
47. Chan H, Cougnard-Grégoire A, Korobelnik JF, et al. Screening for retinopathy of prematurity by telemedicine in a tertiary level neonatal intensive care unit in France: review of a six-year period. *J Fr Ophtalmol*. 2018;41(10):926–932. doi:10.1016/J.JFO.2018.02.020.
48. Yau GSK, Lee JWY, Tam VTY, et al. Incidence and risk factors of retinopathy of prematurity from 2 neonatal intensive care units in a Hong Kong Chinese population. *Asia-Pacif J Ophthalmol*. 2016;5(3):185–191. doi:10.1097/APO.0000000000000167.
49. Hellström A, Hård AL, Engström E, et al. Early weight gain predicts retinopathy in preterm infants: new, simple, efficient approach to screening. *Pediatrics*. 2009;123(4):e638–e645. doi:10.1542/PEDS.2008-2697.
50. Smith LEH, Shen W, Perruzzi C, et al. Regulation of vascular endothelial growth factor-dependent retinal neovascularization by insulin-like growth factor-1 receptor. *Nat Med*. 1999;5(12):1390–1395. doi:10.1038/70963.
51. Chalam KV, Lin S, Murthy RK, Brar VS, Gupta SK, Radhakrishnan R. Evaluation of modified retinopathy of prematurity screening guidelines using birth weight as the sole inclusion criterion. *Middle East Afr J Ophthalmol*. 2011;18(3):214–219. doi:10.4103/0974-9233.84048.
52. Sauer L, Chandler M, Hartnett ME. Extending peripheral retinal vascularization in retinopathy of prematurity through regulation of VEGF signaling. *Am J Ophthalmol*. 2024;260:190–199. doi:10.1016/J.AJO.2023.12.008.
53. Moisseiev E, Waisbourd M, Ben-Artsi E, et al. Pharmacokinetics of bevacizumab after topical and intravitreal administration in human eyes. *Graefes Arch Clin Exp Ophthalmol*. 2014;252(2):331–337. doi:10.1007/S00417-013-2495-0.
54. Zhu Q, Ziemssen F, Henke-Fahle S, et al. Vitreous levels of bevacizumab and vascular endothelial growth factor-A in patients with choroidal neovascularization. *Ophthalmology*. 2008;115(10):1750–1755 1755.e1. doi:10.1016/J.OPHTHA.2008.04.023.
55. Hanif AM, Gensure RH, Scruggs BA, Anderson J, Chiang MF, Campbell JP. Prevalence of persistent avascular retina in untreated children with a history of retinopathy of prematurity screening. *J AAPOS*. 2022;26(1):29–31. doi:10.1016/J.JAAPOS.2021.09.004.
56. Vural A, Ekinci DY, Onur IU, Hergünsel GO, Yiğit FU. Comparison of fluorescein angiographic findings in type 1 and type 2 retinopathy of prematurity with intravitreal bevacizumab monotherapy and spontaneous regression. *Int Ophthalmol*. 2019;39(10):2267–2274. doi:10.1007/S10792-018-01064-7/FIGURES/4.
57. Hartnett ME, Sciences V, Moran JA. Discovering mechanisms in the changing and diverse pathology of retinopathy of prematurity: the Weisenfeld Award Lecture. *Invest Ophthalmol Vis Sci*. 2019;60(5):1286–1297. doi:10.1167/IOVS.18-25525.
58. Simmons AB, Bretz CA, Wang H, et al. Gene therapy knockdown of VEGFR2 in retinal endothelial cells to treat retinopathy. *Angiogenesis*. 2018;21(4):751–764. doi:10.1007/S10456-018-9618-5/FIGURES/7.
59. Zeng G, Taylor SM, McColm JR, et al. Orientation of endothelial cell division is regulated by VEGF signaling during blood vessel formation. *Blood*. 2007;109(4):1345–1352. doi:10.1182/BLOOD-2006-07-037952.